Image Denoising Method Based on Curvelet Transform in Telemedicine

Yang Yu[1], Dan Li[1(✉)], Likai Wang[2], Weiwei Liu[2], Kailiang Zhang[1], and Yuan An[1]

[1] Xuzhou University of Technology, Xuzhou 221000, Jiangsu, China
[2] Traffic Police Detachment of Xuzhou Public Security Bureau, Xuzhou 221000, Jiangsu, China

Abstract. To resolve the problems that the traditional image denoising methods are easy to lose details such as edges and textures, a new method of image denoising was proposed. It based on the Curvelet denoising algorithm, using polynomial interpolation threshold method, combining with Wrapping and Cycle spinning techniques to determine the adaptive threshold of each Curvelet coefficient for denoising the medical images. Simulation experiments confirm that the new method reduces the pseudo Gibbs phenomenon, retains the details and texture of the image better, and obtains better visual effects and higher PSNR values.

Keywords: Curvelet transform · Cyclic translation · Image denoising · Telemedicine

1 Introduction

Images are noisy after acquisition and remote network transmission, which affects the visual and application effects [1–3]. Noise in images has greatly affected people's extraction of information from images, such as medical images, remote sensing images, and computer vision images. In many fields such as medicine and scientific, the requirements for image quality have become higher and higher [4]. Therefore, we need to explore from various angles to improve the quality of the image.

In the field of image denoising, people continue to improve the use of wavelet transform for image denoising [5–7]. The theory of wavelet denoising is still developing. Research is made on transform methods by selecting different basis functions or using frames to transform non-decimating wavelet transforms or selecting the optimal basis to transform the wavelet packets. Wavelet can not express Linear Singularity sparsely and can only be applied to isotropic singular objects. It can't fully study the geometric characteristics of objects, such as the edge, contour and other main features of two-dimensional image, which are the most interesting places for people.

E.J.Candes and D.L.Donoho established a multi-scale method particularly suitable for representing anisotropic singularities-Ridgelet transform based on wavelet theory [8, 9]. It has a strong ability of direction selection and discrimination, but for image denoising of curve singularity, Ridgelet transformation needs to be carried out in blocks. In order to further express the more general curve singularity of multi-dimensional

H. Song and D. Jiang (Eds.): SIMUtools 2020, LNICST 370, pp. 679–690, 2021.
https://doi.org/10.1007/978-3-030-72795-6_54

signals, on the basis of Ridgelet transformation, the local Ridgelet transformation and Curvelet curve transformation methods ware proposed to solve the curve singularity, local straight lines with multiple scales are used to approximate the entire curve.

The first generation of Curvelet is a multi-scale pyramid, which has many direction and location elements in each scale. Its construction idea is to treat the curve as a straight line in each block through a small enough block, and then use the local analysis of its characteristics. E.J.Candes and D.L.Donoho proposed the second-generation Curvelet transform theory, which is completely different in structure from the first generation Curvelet transform [10, 11]. The second generation of Curvelet is a new method based on frequency domain. It no longer uses different scales to decompose objects, no longer analyzes them in blocks, directly analyzes them in frequency domain. It also has high anisotropic characteristics. It can accurately and effectively express important information such as image edges with less non-zero coefficients, and it also has high approximation accuracy for images and better sparse expression ability, which makes the implementation simpler, faster, easier to understand, and the redundancy is greatly reduced.

At present, telemedicine provides a broader development space for the application of modern medicine [12–15]. Telemedicine technology has developed from the initial TV monitoring and telephone remote diagnosis to the comprehensive transmission of digital, image and voice using high-speed network, and realized the communication of real-time voice and high-definition image [16–18]. In this paper, the second-generation Curvelet transform is applied to image denoising. Based on this, existing algorithms are improved to make the image signal-to-noise ratio higher, and the image display effect is more real and clear.

2 Fast Discrete Curvelet Transform

Applying the Curvelet transform to image processing requires its discrete form. Compared with other traditional multi-scale transform (such as wavelet transform) [19–21], the discrete Curvelet transform is a new multi-scale analysis method [22–26], which has obvious advantages in the expression of image edge direction features, and the anisotropic features can better describe the edge and detail of the image [27, 28].

In the Cartesian coordinate system, $f[t_1, t_2]$, $'0 \leq t_1, t_2 \leq n$ is the input, and the discrete form of the Curvelet transform can be expressed as:

$$c^D(j, l, k) := \sum_{0 \leq t_1, t_2 < n} f[t_1, t_2] \overline{\varphi^D_{j,l,k}[t_1, t_2]} \tag{1}$$

Where j, k, l represent the scale, direction, and position respectively, using a bandpass function:

$$\Psi(\omega_1) = \sqrt{\phi(\omega_1/2)^2 - \phi(\omega_1)^2} \tag{2}$$

Definition $\Psi_j(\omega_1) = \Psi(2^{-j}\omega_1)$, using this function to achieve multi-scale segmentation. For each $\omega = (\omega_1, \omega_2)$,$\omega_1 > 0$, corner window is:

$$V_j(S_{\theta_l}\omega) = V(2^{\lfloor j/2 \rfloor}\frac{\omega_2}{\omega_1} - l) \tag{3}$$

$S_{\theta l}$ is a shear matrix.

$$S_{\theta l} := \begin{pmatrix} 1 & 0 \\ -\tan\theta_l & 1 \end{pmatrix} \tag{4}$$

θ_1 is not equally spaced, but the slope is equally spaced. Delimiting $\widetilde{U}_j(\omega) := \psi_j(\omega_1)V_j(\omega)$, for each $\theta_1 \in [-\pi/4, \pi/4)$, it has

$$\widetilde{U}_{j,1}(\omega) := \psi_j(\omega_1)V_j(S_{\theta_1}\omega) = \widetilde{U}_{j,1}(S_{\theta_1}\omega) \tag{5}$$

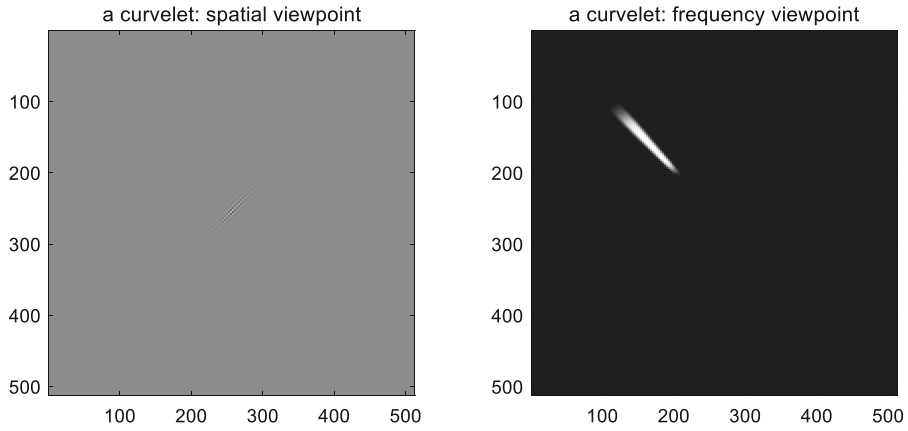

Fig. 1. Spatial and frequency domain maps of scale j

The discrete Curvelet transform method first transforms into the frequency domain and then localizes it in the frequency domain. After localization, the inverse two-dimensional fast Fourier transform is used to obtain the curve coefficient. Figure 1 is a spatial and frequency domain image where the scale is *j*. There are two discrete Curvelet transform algorithms. The first is the discrete Curvelet transform algorithm USFFT (Unequally-Space Fast Fourier Transform) based on fast Fourier transform in non-equivalent space. The second is the fast discrete Curvelet transform algorithm based on wrapping.

2.1 Fast Discrete Curvelet Transform Based on USFFT

The fast discrete Curvelet transform method based on USFFT first transforms the frequency domain [29–32], then localizes in the frequency domain, and then uses two-dimensional Fourier transform after localization. The implementation processes of USFFT are as follows:

Step1: For a given two-dimensional function $f[t_1, t_2]$, $0 \leq t_1, t_2 \leq \omega$ in Cartesian coordinates, performing 2DFFT(Two-Dimensional Fast Fourier Transform), to get a two-dimensional frequency domain representation:

$$\hat{f}[n_1, n_2], \ -n/2 \leq n_1, \ n_2 \leq n/2 \tag{6}$$

Step2: In the frequency domain, for each pair (j, l), j is scale, l is angle, re-sampling $\hat{f}[n_1, n_2]$, getting sampled value $\hat{f}[n_1, n_2 - n_1 \tan\theta_1]$,$(n_1, n_2) \in P_j$, among them,

$$P_j = \{(n_1, n_2) : n_{1,0} \leq n_1 < n_{1,0} + L_{1,j}, n_{2,0} \leq n_2 < n_{2,0} + L_{2,j}\} \tag{7}$$

$L_{1,j}$ and $L_{2,j}$ are the length and width components of the support interval of the window function $\tilde{U}_j[n_1, n_2]$.

Step3: Multiplying the interpolated $\hat{f}$ by the window function $\tilde{U}_j$:

$$\tilde{U}_{j,1}[n_1, n_2] = \hat{f}[n_1, n_2 - n_1 \tan\theta_1]\tilde{U}_j[n_1, n_2] \tag{8}$$

Step4: Performing 2DIFFT inverse transform on $\tilde{f}_{j,1}$, we get a discrete set of curve coefficients $C^D(j, l, k)$.

Mathematically speaking, localization and 2D FFT can be combined into one step, which is to multiply the local Fourier transform basis by the localization window.

2.2 Fast Discrete Curvelet Transform Based on Wrapping

The core idea of fast discrete Curvelet transform based on Wrapping [33–35] is to wrap around the origin, that is to say, in the specific implementation, any area is mapped to the affine area of the origin one by one through periodic techniques. Curvelet wrapping wave is shown in Fig. 2.

The algorithm processes are as the follows:

Step1: Fourier transform of two-dimensional image data in a Cartesian coordinate, to get a frequency domain representation $\hat{f}[n_1, n_2]$,$-n/2 \leq n_1$,$n_2 \leq n/2$.

Step2: For each scale and direction parameter (j, l), interpolation method is used to obtain $\hat{f}[n_1, n_2 - n_1 \tan\theta_1]$ for $\hat{f}[n_1, n_2]$.

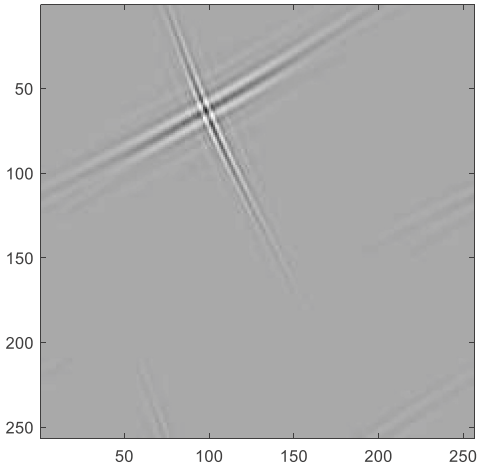

Fig. 2. Curvelet wrapping_wave

Step3: Multiply $\hat{f}$ with the fitting window $\hat{U}_j$ to get $\tilde{f}_{j,l}$.

$$\hat{f}_{j,l}[n_1, n_2] = \hat{f}[n_1, n_2 - n_1 \tan\theta_1]\tilde{U}_j[n_1, n_2] \tag{9}$$

Step4: Wrapping around the origin, localizing $\hat{f}$.

Step5: Inversing $\tilde{f}_{j,l}$ with 2DFFT, this gives the discrete Curvelet coefficient set $C^D(j, l, k)$, *j, l, k* represent the scale, direction, and matrix coordinates of each direction.

These two fast discrete Curvelet transform algorithms have the same output, but the latter is faster and more efficient. When the edge contour direction is consistent with the direction of the Curvelet wave, there will be a large Curvelet coefficient. Otherwise, the Curvelet coefficient is close to zero. When the speckle noise or debris that is much smaller than the target object which appears in the image, applying the Curvelet transform not only makes it easy to filter it out, but also does not lose edge details, which is helpful for accurate edge extraction.

3 Improved Image Denoising Algorithm

According to the Curvelet transform theory, a larger Curvelet coefficient corresponds to a stronger edge, and a noise corresponds to a smaller coefficient. Although the threshold method can be used to obtain a good denoising effect and local features such as image edge can be retained well, it will cause visual distortion such as ringing, pseudo Gibbs effect [36, 37]. So the image display effect is not ideal. The hard threshold function will lose a lot of detailed information in the denoised image, because the hard threshold is discontinuous at the threshold point, which will overkill the transform coefficients. Although the soft threshold function has good overall continuity, it is an amount that

subtracts a threshold from the original coefficient, which directly affects the degree of approximation of the reconstructed signal to the real signal. The derivative of the soft threshold function is not continuous, but we need to operate on the first derivative, second derivative or higher derivative of the signal, and the soft threshold is not suitable for this case. Based on the above considerations, in order to obtain better medical visual effect and reduce the noise caused by long-distance transmission [38–40], this paper uses a polynomial interpolation method based on the hard threshold to improve the denoising algorithm.

Define p (x) as a cubic polynomial:

$$P(x) = R_0x^3 + R_1x^2 + R_2x + R_3 \tag{10}$$

The improved threshold function expression is:

$$\hat{w} = \begin{cases} w, |w| > \lambda_2 \\ sign(w)P(w), \lambda_1 \le |w| \le \lambda_2 \\ 0, |w| < \lambda_1 \end{cases} \tag{11}$$

From the continuous and differentiable properties, the following relationship is obtained:

$$P(\lambda_1) = 0, P(\lambda_2) = \lambda_2, \ P'(\lambda_1) = 0, P'(\lambda_2) = 1 \tag{12}$$

The cubic function has high-order differentiability.

$$P(x) = \frac{\lambda_1+\lambda_2}{(\lambda_1-\lambda_2)^3}x^3 - \frac{2\lambda_1^2+2\lambda_1\lambda_2+2\lambda_2^2}{(\lambda_1-\lambda_2)^3}x^2 + \frac{\lambda_1^3+\lambda_1^2\lambda_2+4\lambda_1\lambda_2^2}{(\lambda_1-\lambda_2)^3}x - \frac{2\lambda_1^2\lambda_2^2}{(\lambda_1-\lambda_2)^3} \tag{13}$$

Where λ_1, λ_2 meet the conditions: $0 < \lambda_1 < \lambda < \lambda_2$. Interpolating with a cubic polynomial in the interval $\lambda_1 \le |w| \le \lambda_2$, the improved threshold function is continuous and differentiable at λ_1, λ_2. The threshold function is continuous as a whole and has high-order derivability. λ_1,λ_2 can be selected according to actual needs. When the values of λ_1 and λ_2 are almost equal, the threshold function is the hard threshold function. In addition, adjusting λ_2 when it is greater than the threshold can keep the details well, which overcomes the defect of soft threshold to some extent, so it has the incomparable flexibility of soft and hard threshold function.

In order to suppress the pseudo Gibbs phenomenon caused by the lack of invariance of the transformation during the threshold denoising process, this paper uses a translation image to change the position of the discontinuous points. The Cycle spinning method performs cyclic translation on the signal. This method first performs cyclic translation on the noisy signal, then performs threshold denoising, and finally performs reverse cyclic translation.

Suppose the translation is $(i, j), i \in (0, M), j \in (0, N)$, M and N are image width and height. After each translation denoising, we will get a result $Y_{i,j}$, the two-dimensional image can translate the row and column at the same time. The linear average of the denoising results can suppress the pseudo Gibbs phenomenon and get the denoising image $\hat{Y}(i, j)$. The specific process is shown in the following formula:

$$\hat{Y}(i,j) = \frac{1}{K_1 K_2} \sum_{i=1,j=1}^{K_1 K_2} Y_{-i,-j}(F^{-1}(T[F(Y_{i,j})])) \tag{14}$$

In the above formula, K_1, K_2 are the maximum translation of rows and columns. Full translation is based on the entire signal length. T is the threshold, F and F^{-1} are wavelet transform and inverse transform, $Y_{i,j}$ represents panning the image. $Y_{-i,-j}$ represents the opposite translation operation after denoising. This method can well suppress the pseudo Gibbs phenomenon. The translation invariant wavelet denoising method can also reduce the RMSE(Root Mean Square Error) between the original signal and the estimated signal.

In this paper, based on the Curvelet transform, combining the Wrapping method and Cycle spinning, the pseudo Gibbs effect is suppressed, and the improved polynomial interpolation threshold function method is used to denoise. The specific methods are as follows:

Step1: The noisy image is cyclically translated with a translation amount of 1. The translation method is as described above.

Step2: The Wrapping-based Curvelet transform is performed on the translated image to obtain the discrete Curvelet coefficient set $C^D(j, l, k)$ at all scales and directions.

Step3: The improved polynomial interpolation thresholding function is used to denoise the Curvelet coefficients at different scales and directions.

Step4: Performing Curvelet inverse transform, and translate to reconstruct the image to get the denoised image.

Step5: Reverse cycle translation of denoised image, repeat the above steps and average the results after iteration, and the final denoising result $x(i, j)$ is obtained.

This method can not only effectively remove the pseudo Gibbs phenomenon and show better surface quality, but also can obtain smaller RMSE and improve the signal-to-noise ratio.

4 Simulation Experiment and Performance Analysis

In order to test the superiority of the new denoising algorithm, we selected a human lung medical image with a size of 256×256 for experiments in the Matelab2018 environment. The original image is shown in Fig. 3. Figure 4 is a comparison of Wrap Curvelet and the new algorithm in different noise standard deviations of 5, 10, 15, 20, and 30. Table 1 is the results of PSNR under different noise standard deviations. Test methods include: mean filtering denoising, wavelet threshold denoising, Wrap Curvelet algorithm denoising and denoising algorithm of this paper.

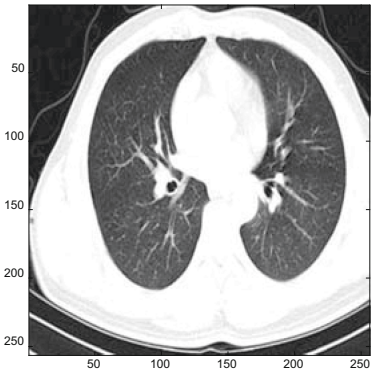

Fig. 3. The original image

As shown in Fig. 4, compared with Wrap Curvelet, the algorithm of this paper has a clearer image of different noise standard deviation. The new algorithm can better restore the texture in the image, and retains the edge information better with different noise standard deviation.

As shown in Table 1, from the perspective of PSNR, among the four denoising methods, wavelet threshold based method is better than mean filtering, and Wrap Curvelet based method is better than wavelet threshold method. Combined with other algorithms, the new algorithm has the highest PSNR value, better reduces the pseudo Gibbs phenomenon and ringing effect in the image. It also reduces the RMSE of the signal, better preserves the high frequency details and texture of the image.

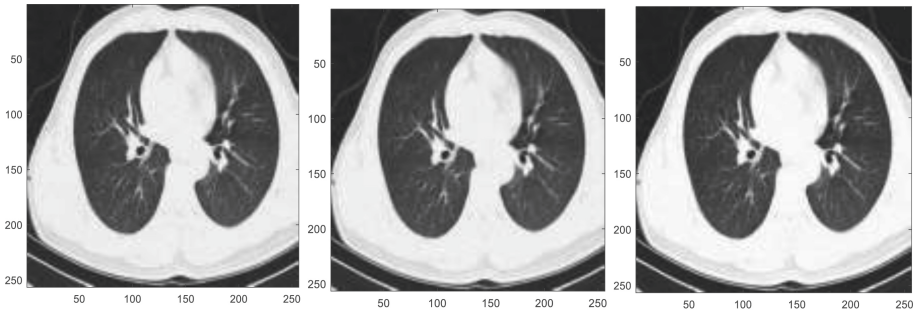

(a)SD=5 (b)Wrap Curvelet denoising (c)The paper denoising

Fig. 4. Comparison of denoising results of different algorithms

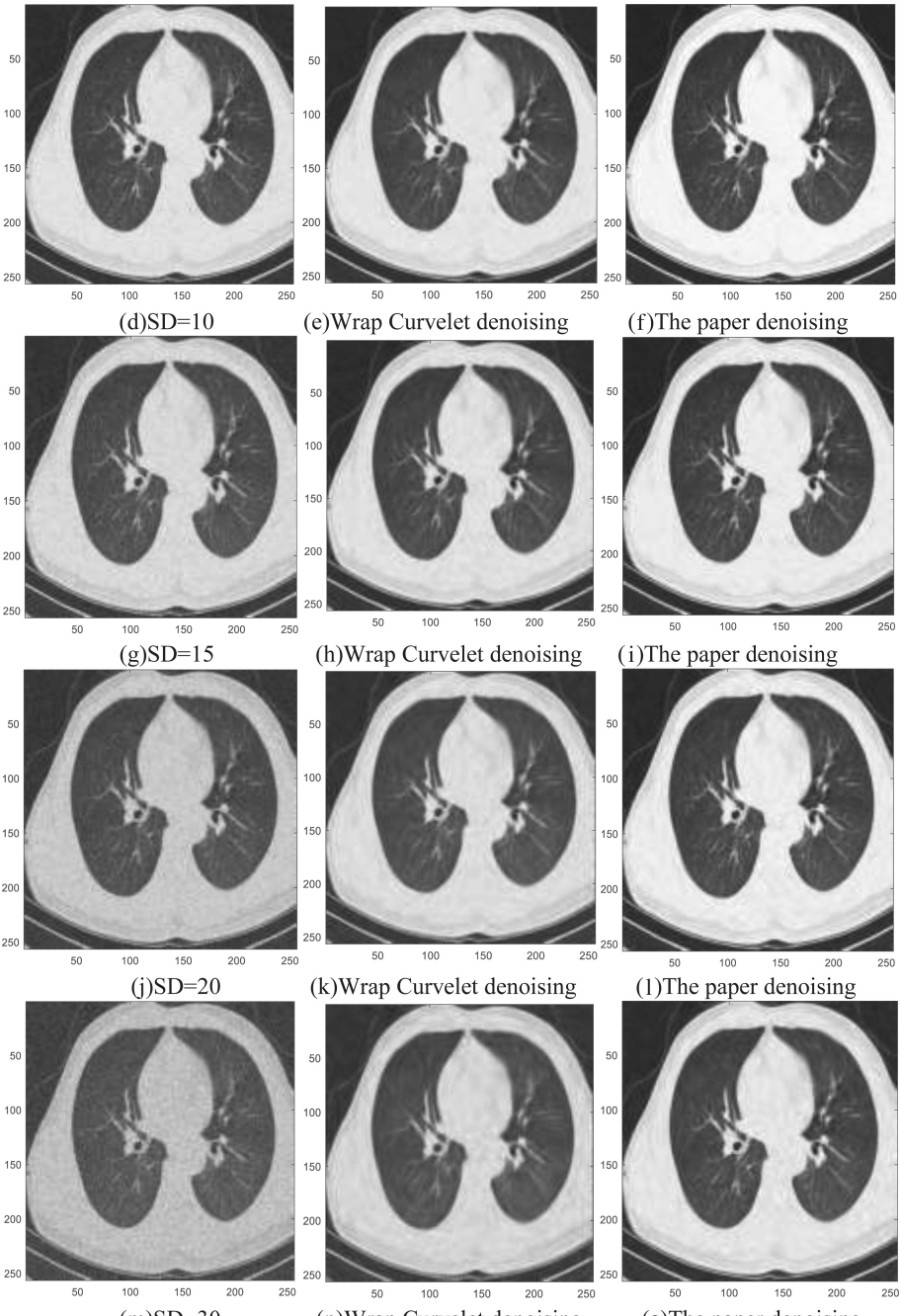

Fig. 4. (*continued*)

Table 1. Comparison PSNR with different algorithms in different SD

Standard deviation of noise	Before noise reduction	Mean filtering	Wavelet threshold	Wrap curvelet	This paper
5	31.1235	31.4453	31.8456	32.3592	36.4286
10	28.1703	29.0435	29.5667	29.7805	32.6237
25	24.587	25.1864	26.6482	27.9592	30.5172
20	22.1149	23.8642	25.1867	26.6603	29.0218
30	18.6075	22.5378	24.5753	25.1131	27.1014

5 Conclusion

Traditional medical image denoising is processed in the spatial or frequency domain. However, noise, edges and pixel points on the contour are located in places where the grayscale changes abruptly. They all correspond to the high frequency components in the image spectrum. Therefore, the image processed by the traditional noise reduction methods are likely to make the details, such as edge contours, lines blurred. So that the image quality can be reduced. In order to reduce the shortcomings of losing edges and textures details, this paper proposes an improved image denoising algorithm based on Curvelet transform. Polynomial interpolation threshold method is used in this algorithm, Wrapping and Cycle spinning technology are combined, the Curvelet coefficient threshold can be determined adaptively, so as to achieve the denoising of medical images. The experiments show that the algorithm in this paper has a good effect on the suppression of medical image noise, and has good subjective vision. It can improve the shortcomings of the image acquisition by instrument and remote transmission, it has practical application significance.

Acknowledgement. This work is partly supported by the Science and Technology Project of Jiangsu Provincial Department of Housing and Construction (2019ZD039), Science and Technology Project of Jiangsu Provincial Department of Housing and Construction (2019ZD040).

References

1. Papyan, V., Elad, V.: Multi-scale patch-based image restoration. IEEE Trans. Image Process. **25**(1), 249–261 (2016)
2. Jiang, D., Wang, Y., Lv, Z., Wang, W., Wang, H.: An energy-efficient networking approach in cloud services for IIoT networks. IEEE J. Sel. Areas Commu-n. **38**(5), 928–941 (2020)
3. Jiang, D., Huo, L., Song, H.: Rethinking behaviors and activities of base stations in mobile cellular networks based on big data analysis. IEEE Trans. Netw. Sci. Eng. **7**(1), 80–90 (2020)
4. Somasundaran, B.V., Soundararajan, R., Biswas, S.: Image denoising for image retrieval by casscading a deep quality assessment network. In: 25th IEEE International Conference on Image Processing (ICIP), pp. 525–529. IEEE (2017) https://doi.org/10.1109/ICIP.2018.8451132

5. Ding, Y., Selesnick, I.W.: Artifact-free wavelet denoising: non-convex sparse regularization, Convex Optimization. IEEE Trans. Signal Process. **22**(9), 1364–1368 (2015)
6. Wu, Y., Gao, G., Cui, C.: Improved wavelet denoising by non-convex sparse regularization under double wavelet domains. IEEE Access **7**, 30659–30671 (2019)
7. Li, D., Xiao, L.Q., Tian, J., Sun, J.P.: Mine image stitching based on invariant feature and lifting wavelet. J. Chin. Comput. Syst. **35**(07), 1671–1675 (2014)
8. Candes, E.J.: Ridgelet: theory and applications. Department of Statistics, Stanford University, USA (1998)
9. Mangaiyarkarasi, P., Arulselvi, S.: A new digital image watermarking based on Finite Ridgelet Transform and extraction using ICA. In: International Conference on Emerging Trends in Electrical and Computer Technology, pp. 837–841 (2011)
10. Mahdinejad, N., Mota, H.O., Silva, E.J., Adriano, R.: Improvement of system quality in a generalized finite-element method using the discrete curvelet transform. IEEE Trans. Magn. **53**(6), 1–4 (2017). https://doi.org/10.1109/TMAG.2017.2659652
11. Guo, J.M., Prasetyo, H., Farfoura, M.E., Lee, H.: Vehicle verification using features from curvelet transform and generalized gaussian distribution modeling. IEEE Trans. Intell. Transp. Syst. **16**(4), 1989–1998 (2015)
12. Jeng-Miller, K.W., Yonekawa, Y.: Telemedicine and pediatric retinal disease. Int. Ophthalmol. Clin. **60**(1), 47–56 (2020)
13. Ray, K.N., Mehrotra, A., Yabes, J.G., Kahn, J.M.: Telemedicine and outpatient subspecialty visits among pediatric medicaid beneficiaries. Acad. Pediatr. **20**(5), 642–651 (2020)
14. Huo, L., et al.: An intelligent optimization-based traffic information acquirement approach to software-defined networking. Comput. Intell. **36**(1), 151–171 (2019)
15. Hernando-Requejo, V., Huertas-González, N., Lapeña-Motilva, J., Ogando-Durán, G.: The epilepsy unit during the covid-19 epidemic: the role of telemedicine and the effects of confinement on patients with epilepsy. Neurología (English Edition) **35**(4), 274–276 (2020)
16. Wang, F., Jiang, D., Qi, S.: An adaptive routing algorithm for integrated information networks. China Commun. **7**(1), 196–207 (2019)
17. Huo, L., et al.: An AI-based adaptive cognitive modeling and measurement method of network traffic for EIS. Mob. Netw. Appl. pp. 1–11 (2019)
18. Jiang, D., et al.: Big data analysis based network behavior insight of cellular networks for industry 4.0 applications. IEEE Trans. Ind. Inform. **16**(2), 1310–1320 (2020)
19. Liu, Y., Liu, S., Wang, Z.: A general framework for image fusion based on multi-scale transform and sparse representation. Inf. Fusion. **24**, 147–164 (2015)
20. Jiang, D., Huo, L., Li, Y.: Fine-granularity inference and estimations to network traffic for SDN. PLoS ONE **13**(5), 1–23 (2018)
21. Hardalac, F., Yaşar, H., Akyel, A., Kutbay, U.: A novel comparative study using multi-resolution transforms and convolutional neural network (cnn) for contactless palm print verification and identification. Multimedia Tool Appl. **79**, 22929–22963 (2020)
22. Ja'Afar, N.H.: Implementation of fast discrete curvelet transform using field-programmable gate array. Int. J. Adv. Trends Comput. Sci. Eng. **9**(1.2), 167–173 (2020)
23. Vyas, R., Kanumuri, T., Sheoran, G., Dubey, P.: Efficient iris recognition through curvelet transform and polynomial fitting. Optik **185**, 859–867 (2019)
24. Jiang, D., Zhang, P., Lv, Z., et al.: Energy-efficient multi-constraint ligent optimization-brouting algorithm with load balancing for smart city applications. IEEE Internet Things J. **3**(6), 1437–1447 (2016)
25. Jiang, D., Li, W., Lv, H.: An energy-efficient cooperative multicast routing in multi-hop wireless networks for smart medical applications. Neurocomputing **220**, 160–169 (2017)
26. Khadilkar, S.P., Das, S.R., Assaf, M.H., Biswas, S.N.: Face identification based on discrete wavelet transform and neural networks. Int. J. Image Graph. **19**(04), 634–654 (2019)

27. Mahdinejad, N., Mota, H.O., Silva, E.J., Adriano, R.: Improvement of system quality in a generalized finite-element method using the discrete curvelet transform. IEEE Trans. Magn. **53**(6) 1–4 (2017)
28. Yang, Y., Tong, S., Huang, S.Y., Lin, P., Fang, Y.M.: A hybrid method for multi-focus image fusion based on fast discrete curvelet transform. IEEE Access **5**, 14898–14913 (2017)
29. Ahmed, R., Riaz, M.M., Ghafoor, A.: Attack resistant watermarking technique based on fast curvelet transform and robust principal component analysis. Multimedia Tool Appl. **77**(8), 9443–9453 (2018)
30. Wang, K., Yang, X., Tian, Z., Du, T.: The finger vein recognition based on curvelet. In: Proceedings of the 33rd Chinese Control Conference, pp. 4706–4711. IEEE (2014)
31. Wang, Y., Jiang, D., Huo, L., Zhao, Y.: A new traffic prediction algorithm to software defined networking. Mob. Netw. Appl. pp. 1–10 (2019)
32. Chaki, J., Parekh, R., Bhattacharya, S.: Plant leaf recognition using texture and shape features with neural classifiers. Pattern Recogn. Lett. **58**, 61–68 (2015)
33. Agrawal, D., Karar, V.: Generation of enhanced information image using curvelet-transform-based image fusion for improving situation awareness of observer during surveillance. Int. J. Image Data Fusion **10**(1), 45–57 (2019)
34. Qi, S., Jiang, D., Huo, L.: A prediction approach to end-to-end traffic in space information networks. Mob. Netw. Appl. 1–10 (2019)
35. Elnemr, H., Elnemr, H.A.: Color histogram with curvelet and cedd for content-based image retrieval. Int. J. Comput. Inf. Secur. **15**(12) (2018)
36. Sharif, B., Dharmakumar, R., Labounty, T., Arsanjani, R., Shufelt, C., Thomson, L., et al.: Towards elimination of the dark-rim artifact in first-pass myocardial perfusion mri: removing gibbs ringing effects using optimized radial imaging. Magn. Reson. Med. **72**(1), 124–136 (2014)
37. Veraart, J., Fieremans, E., Jelescu, I.O., Knoll, F., Novikov, D.S.: Gibbs ringing in diffusion MRI. Magn. Reson. Med. **76**(1), 301–314 (2016)
38. Jiang, D., Huo, L., Lv, Z., Song, H., Qin, W.: A joint multi-criteria utility-based network selection approach for vehicle-to-infrastructure networking. IEEE Trans. Intell. Transp. Syst. **19**(10), 3305–3319 (2018)
39. Jiang, D., Wang, W., Shi, L., Song, H.: A compressive sensing-based approach to end-to-end network traffic reconstruction. IEEE Trans. Netw. Sci. Eng. **7**(1), 507–519 (2020)
40. Bitunguhari, L., Manzi, O., Walker, T., Mukiza, J., Clerinx, J.: Pathological features seen on medical imaging in hospitalized patients treated for tuberculosis in a reference hospital in rwanda. Rwanda Med. J. **76**(4), 1–9 (2020)